



Effect of enhanced cooling on mechanical properties of a multipass welded martensitic steel

Juhani Laitila¹ · Jari Larkiola¹

Received: 18 September 2018 / Accepted: 3 December 2018 / Published online: 3 January 2019
© The Author(s) 2019

Abstract

The effect of forced cooling using heat sinks on the mechanical properties and interpass waiting time of two-pass welds has been studied for a martensitic steel with a yield strength of 960 MPa when the interpass temperature was 100 °C. Cross-weld tensile and –40 °C Charpy-V impact toughness properties were examined. The use of heat sinks is shown to result in a beneficial increase of the cross-weld yield strength but at the expense of the yield-to-tensile strength ratio. Due to its particularly detrimental effect on the heat-affected zone (HAZ) toughness of multipass welds, special attention was given in the Charpy-V toughness of the intercritically reheated coarse-grained HAZ (ICCGHAZ) by also testing simulated ICCGHAZs. It is shown that forced cooling has a beneficial effect in respect of the toughness of this simulated subzone and on the Charpy-V toughness of the HAZ of the actual welds. The interpass cooling time during the two-pass welding was reduced by 37%. The results indicate that, in the case of high-strength steels, it may be possible to simultaneously improve both welding productivity and mechanical properties by using forced cooling down to 100 °C to reduce waiting time between weld passes.

Keywords Arc welding · GMAW · Martensite · ICCGHAZ · Cooling time

1 Introduction

Nowadays, high- and ultrahigh-strength steels have become common in different applications such as skyscrapers, bridges, cars, cranes, and pipelines and in other applications in which it is desired to minimize the weight of the structure or to minimize the material cost [1–3]. Often, these steels have low alloying elements to minimize the cost of the steel to make it a more cost-efficient option over other high- or ultrahigh-strength materials such as titanium alloys or maraging steels. Furthermore, low-alloyed high- and ultrahigh-strength steels often have low carbon content as well [1, 4]. However, often, the welding of these low-carbon, low-

alloyed steels is demanding as, unlike traditional structural steels, the welds must cool quickly to avoid loss of cross-weld tensile properties [2]. This is the opposite of traditional steels for which rapid weld cooling can induce hardening and a loss of toughness. For example, one manufacturer recommends cooling times of 13 s or less between 800 and 500 °C ($t_{8/5}$) for a high-strength steel with a tensile strength of 700 MPa [1]. As the strength of the steel increases, the recommended maximum cooling time tends to decrease [4]. Usually, the recommended $t_{8/5}$ for high- and ultrahigh-strength steels is between 4 and 20 s [1, 4].

For decades, $t_{8/5}$ has been used as a guideline for achieving desirable weld quality, as most of the microstructural changes in steel take place in temperatures above 500 °C. However, $t_{8/5}$ does not take into account microstructure transformations such as lower bainite that forms below 500 °C [5]. Regardless of this fact, $t_{8/5}$ can still be used for ultrahigh- and high-strength steels since usually, it relates not only to the time spent on cooling between 800 and 500 °C but also to the whole thermal cycle including the time spent at high temperatures: longer $t_{8/5}$ times are associated with higher heat inputs, which translate into longer times at temperatures above 1000 °C, where austenite grain growth occurs. This, combined with the fact that the tendency to form upper bainite increases

Recommended for publication by Commission IX - Behaviour of Metals
Subjected to Welding

✉ Juhani Laitila
Juhani.Laitila@Oulu.fi

Jari Larkiola
Jari.Larkiola@Oulu.fi

¹ Materials and Production Engineering, Faculty of Technology, University of Oulu, Pentti Kaiteran Katu 1, 90570 Oulu, Finland

with increasing $t_8/5$, leads to the upper limit on $t_8/5$ needed to retain sufficient toughness in the heat-affected zone (HAZ). The lower limit on $t_8/5$ can be set as a precaution against overly high HAZ hardness, which is detrimental with respect to hydrogen cracking and toughness.

Usually, to achieve the recommended maximum $t_8/5$ times, the welding heat input is limited [6]. However, in the case of traditional gas metal arc welding (GMAW), this easily leads to reduced weld metal deposition rates and the need for multipass welding or an increased number of welding passes. Alternatively, heat input can be reduced by using welding methods like laser welding, hybrid welding, friction stir welding (FSW), or pulsed GMAW (P-GMAW). However, laser welding requires very tight tolerances for the seam, and FSW is not a feasible option to be used for high- and ultrahigh-strength steels. This means that heat input is usually limited by using multiple weld passes. P-GMAW could be used also, but normally, GMAW is still the dominant welding method for high- and ultrahigh-strength steel welding.

The reason why the heat input is so crucial is that it has a significant effect on the cooling time of the weld, which affects the final microstructure in the HAZ adjacent to the weld deposit [6]. As the microstructure determines the mechanical properties of the steel, it is important to minimize the negative effects the thermocycle has on the microstructure. The HAZ tends to have larger grain size due to the grain growth caused by elevated temperatures, which, along with carbides and other microstructural changes, is detrimental to the mechanical properties of the weld [7–12]. The HAZ comprises several subzones: the coarse-grained HAZ (CGHAZ), the fine-grained HAZ (FGHAZ), the intercritical HAZ (ICHAZ), the subcritical HAZ (SCHAZ) and, in the case of multipass welds, the intercritically reheated CGHAZ (ICCGHAZ) [7]. Out of these zones, CGHAZ and ICCGHAZ usually have the lowest impact toughness of all the subzones in the weld [7, 9, 12]. The ICCGHAZ is present only in multipass welds because it is produced by reheating the CGHAZ to around 750–850 °C [7]. As every weld pass produces a new ICCGHAZ, the number of brittle zones increases as the number of weld passes increases [7, 9]. This means that it is beneficial to minimize the number of weld passes to minimize the number of local brittle zones (LBZs), which means that the interpass temperature should be low as possible to allow the use of the highest possible arc energy.

Steel manufacturers also provide recommendations for interpass temperatures for both ultrahigh- and high-strength steels, which are between 300 and 100 °C, but if matching weld is desired, the maximum interpass temperature is often 100 °C [4]. The lower the interpass temperature the higher the allowed heat input will be for the next weld pass, which, depending on the material

thickness, can influence the number of weld passes required. Previously, it has been shown that in the case of a high-strength steel with a tensile strength of 550 MPa, an interpass temperature of around 130 °C caused the steel to have optimal mechanical properties [13]. Furthermore, in other study, it was shown that an interpass temperature of around 80 °C produced superior tensile properties compared to higher interpass temperatures [14].

However, waiting for the weld to cool down to 100 °C can take several minutes, meaning that more time can be spent waiting between weld passes than actually welding. The arc time tends to be quite short, especially when beam structures are welded, for example in the case of a 500-mm-long weld, the arc time of one weld pass can be around 1 min. If three weld passes are required for the beam in the example, the total arc time would be around 3 min and the time spent waiting for the weld to cool to the interpass temperature could be nearly 10 min. From a productivity point of view, therefore, it would be beneficial to apply external cooling to reduce the waiting time as much as possible. Furthermore, previous research by the present authors conducted on the CGHAZ of two different steels with yield strengths of 700 and 960 MPa has shown that mechanical properties are strongly affected by the cooling rate below 500 °C [15, 16]. It was discovered that cooling the weld rapidly all the way to 100 °C produced better mechanical property combinations than rapid cooling to 500, 400, 300, or 200 °C followed by free cooling in air. Depending on the steel studied, tensile strength, yield strength, elongation to fracture, and impact toughness either increased or remained unaffected when forced cooling at 15 °C/s to 100 °C rather than higher temperatures or completely free cooling [15, 16]. However, the effect of forced cooling depends on the steel chemistry involved, for example, in one previous study conducted by Hoy et al. demonstrated that six different low-carbon steels became brittle at low temperatures (–40 °C) when they were cooled rapidly to temperatures below 300 °C [17], meaning that those steels cannot be cooled rapidly if they are to be used in cold environments. The cause of the embrittlement was increased quantities of granular bainite (GB) and bainitic ferrite (BF) and the decrease in the quantity of acicular ferrite (AF). GB and BF had larger grain size than AF, which led to the lower toughness [17].

In practice, it is difficult to cool the weld down rapidly to 100 °C. Some possibilities are compressed air, liquid argon, liquid nitrogen, or solid carbon dioxide (CO₂). However, compressed air has a very low cooling potential, while liquid argon and liquid nitrogen are consumed during use making them expensive solutions. When using

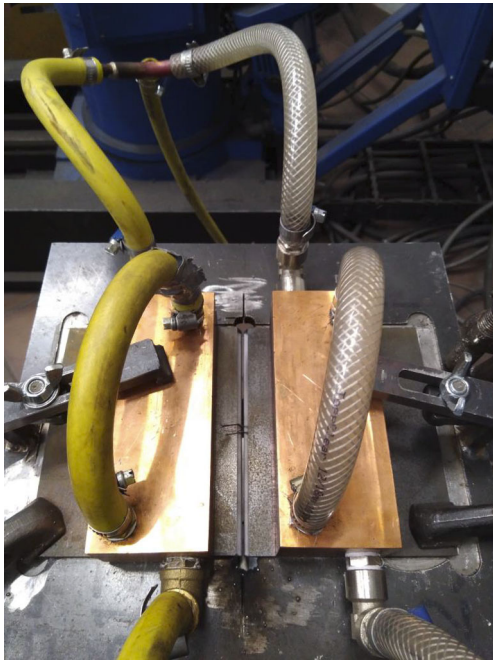


Fig. 1 Welding setting with thermocouple and cooling blocks contacting the upper surface of the plates either side of the weld preparation

solid CO₂, the weld has to be protected from the CO₂ coming into contact with the molten weld pool and it, too, is consumed during use. Consequently, none of the above technologies are cost-effective for the purpose of

Table 1 Chemical composition of steel (wt% max) [19]

C	Si	Mn	P	S	Cr	Al (min %)	Nb	V	Ti
0.12	0.25	1.30	0.020	0.010	0.80	0.015	0.05	0.05	0.07

cooling the whole weld down to an interpass temperature of 100 °C [18]. Therefore, in this study, the cooling

Table 2 Welding parameters used in the experiment

Parameter	Value
Current (I)	240 A
Voltage (U)	22.9 V
Travel speed weld pass 1 (v_1)	600 mm/min
Travel speed weld pass 2 (v_2)	400 mm/min
Angle of the weld torch	17°
Wire feed (f)	6.2 m/min (Aristorod 89, Ø1.2 mm)
Arc energy weld pass 1 (E_1)	0.55 kJ/mm
Heat input weld pass 1 (Q_1)	0.44 kJ/mm
Arc energy weld pass 2 (E_2)	0.82 kJ/mm
Heat input weld pass 2 (Q_2)	0.66 kJ/mm
Gas flow rate	18 l/min (Mison 25)
Preheating temperature (first welding pass)	21 °C

potential of water-cooled copper sinks, meaning water-cooled copper blocks that are placed on top of the steel next to the weld seam, is studied along with the effect the cooling has on the mechanical properties of the weld. In addition, the effect of forced cooling rate on the impact toughness of the ICCGHAZ is studied as the ICCGHAZ is one of the major LBZs caused by multipass welding.

2 Experimental procedures

The experimental part of research was based on multipass welding experiments carried out with a Kemppi Pro MIG 500, together with Motoman-yasnac RX robot and water cooled copper heat sinks. The welding setting can be seen in Fig. 1 and the material composition is shown in Table 1. Furthermore, the welding and cooling parameters are given in Tables 2 and 3. The cooling block dimensions are demonstrated in the Fig. 2 and the welding geometry is shown in Fig. 3. In addition, the properties of the ICCGHAZ microstructure were studied using specimens heat treated on a Gleeble 3800 simulator. The welding parameters can be seen in Tables 2 and 3 and the welding jig in Fig. 1. Two different welding settings were used to analyze the difference between the mechanical properties of welded joints with and without external cooling.

The material used in the welding tests was an 8-mm-thick commercial grade of ultrahigh-strength steel. The material was chosen due to its suitability for the construction industry while having an ultrahigh strength and the fact that it has a mainly martensitic microstructure. The steel has a minimum specified yield strength ($R_{p0.2}$) of 960 MPa, a tensile strength (R_m) in the range 980–1250 MPa, an elongation to fracture (A_5) of at least 7%, and a specified minimum impact strength of 27 J at –40 °C [19]. The chemical composition of the steel as

Table 3 Copper (C110) cooling block parameters

Parameter	Value
Copper block length (l)	150 mm
Copper block width (w)	60 mm
Copper block height (h)	40 mm
Coolant passage diameter (d)	12 mm
Water flow (v)	6 l/min
Water temperature (T)	4 °C
Distance from weld	13 mm

given by the manufacturer is shown in Table 1. The manufacturer’s recommended cooling time $t_{8/5}$ for the steel is from 5 to 15 s [19].

The orientation of the welds was such that cross-weld tensile specimens and Charpy V-notch specimens were transverse to the rolling direction. Furthermore, the Charpy specimens that were cut out of the welded joint were etched, and the notch was positioned in such a way that the fusion line was in the middle of the notch. Additional Charpy specimens were made by using Gleeble to achieve ICCGHAZ specimens to study the impact of the cooling has on the toughness of ICCGHAZ. For each type of specimens and for each parameter, three specimens were used. Furthermore, in the case of tensile strength specimens and Charpy-V specimens that were made out of the welded joint, one specimen of each type was taken from one weld.

The Charpy specimens cut from the welded joint were taken from 29 and 42 mm from the end of weld, and the tensile specimens were cut 36 mm from the beginning of the weld. The specimens were water jet cut to avoid

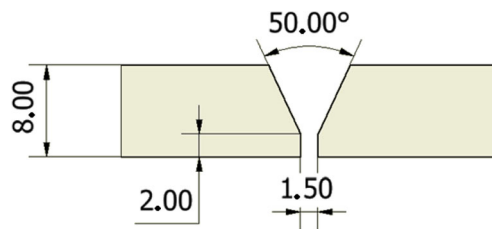
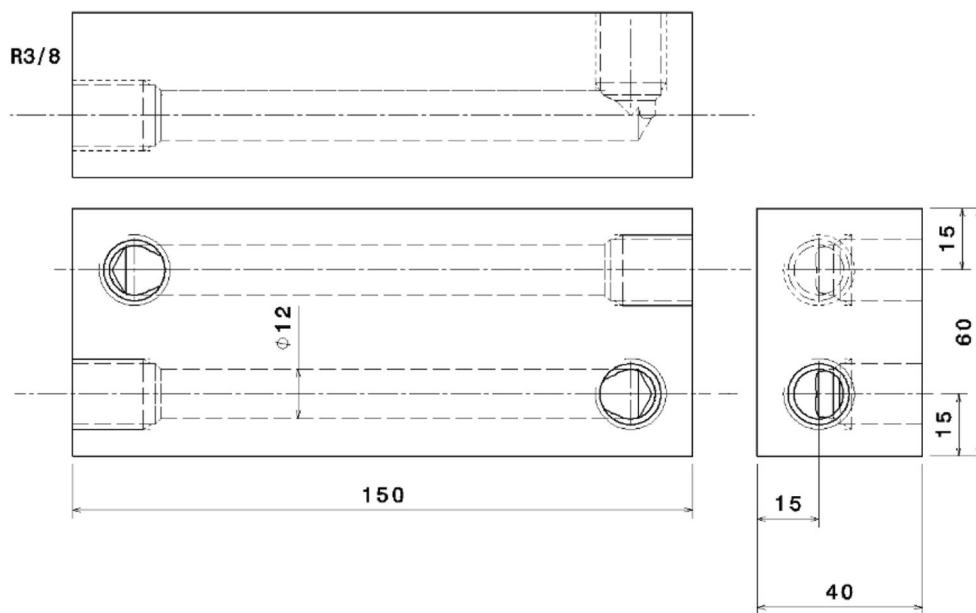


Fig. 3 Weld seam dimensions (mm)

changes in the temperature of the steel. After the cutting, samples were machined to fulfill the required tolerance of the standard EN 10045-1 for the $55 \times 10 \times 5$ mm subsize Charpy V-notch specimens. Testing was made according to EN 10045-1 at -40 °C. After testing, ductile fracture percentages were evaluated in accordance with ISO 148-1. Cross-weld tensile testing was made using 3-mm-thick flat specimens that were obtained from the 8-mm-thick welded sheets by milling away 2.5 mm from the weld face side and 2.5 mm from the root side. The specimens had a width of 12 mm in the 75-mm-long reduced section with the weld at its middle. The gauge length used was 50 mm.

The plates that were welded had dimensions of $145 \times 120 \times 8$ mm, 145 mm being the length of the weld, and the weld preparation comprised a V-joint with an angle of 50° , an air gap of 1.5 mm, and a root height of 2 mm. The temperature of the weld was measured at the middle of the weld length, as shown in Fig. 1. The type of thermocouple used was K20-2-350 which has a maximum temperature limit of 1200 °C. As the measured temperatures in these experiments were between 800 and 100 °C, the thermoelement chosen was adequate for the task. The point from which the temperature was

Fig. 2 Cooling block technical drawing (mm)



measured from in this experiment was the bottom of the weld. The frequency used in the temperature measurement was 10 Hz.

The multipass weld was achieved by using one welding robot program that included both weld passes. However, the program was paused between the weld passes until the temperature of the steel reached 100 °C after which the welding continued. During this pause, the first weld pass was cleaned with a steel brush. Every tensile specimen was taken from a different weld, and in the case of the toughness specimens that were taken from the actual welds, one to two specimens were taken from each welded specimen.

2.1 Gleeble simulations

The cooling time measured with the thermocouples during one of the actual welds was used to do further experiments with a Gleeble. The cooling data can be seen in Tables 4 and 5. The heating speed during the Gleeble experiments was 400 °C/s, and the specimens were held for 1 s at the peak temperatures.

The Gleeble simulation runs were done in series, meaning that as soon as the first Gleeble run cooled down to 100 °C, the next run was initiated. These cycles produce the simulated ICCGHAZ microstructure which is found in multipass welds.

The specimens for microstructural examination were cut from the middle of the Gleeble-simulated specimens. After the microscopic specimens were polished, they were etched with 2% nital. Microstructures were studied using optical microscopy and high-resolution secondary

Table 4 Cooling times for first Gleeble run

Temperature (°C)	Cooled, pass 1 (s)	Normal, pass 1 (s)
1350	0	0
800	2.8	2.8
700	3.8	3.8
600	4.8	5.1
500	7	7.3
450	9.5	10.5
400	12	13.1
350	16	17.1
300	20.6	22.6
250	27.4	30.8
200	38.6	43.4
150	58.6	67
100	93.8	118.6

Table 5 Cooling times for second Gleeble run

Temperature (°C)	Cooled, pass 2 (s)	Normal, pass 2 (s)
750	0	0
600	5	5.2
500	11	11.2
450	16.6	17.6
400	23.4	24.4
350	31.8	32.8
300	42.2	44.6
250	55.8	61.6
200	74.6	87.6
150	104.2	133.2
100	152.6	230

electron imaging (SEI) in a field emission scanning electron microscope (FESEM).

3 Results and discussion

3.1 Cooling rates and times

The thermocycle of the actual welds can be seen in Fig. 4. It is obvious that the cooling blocks do not significantly influence the cooling rates in temperatures above 500 °C. Below 500 °C, the cooled and normal cooling curves start to diverge, and below 300 °C, the cooling rates differ from each other ever more significantly. Furthermore, the cooling rate differences are more profound during the second weld pass as can be expected because of the preheated condition of the steel that is produced by the first weld pass.

Individual cooling times as well as averages for t_{8/5} can be seen in Fig. 5 and t_{8/1} times in Fig. 6. The average differences between cooled and normal times can be seen in Table 6. The cumulative time saving between the normal and cooled welds was 142.1 s on average of which less than 1 s is achieved in temperatures above 500 °C, when two weld passes were used.

3.2 Impact toughness

The impact toughness values of the Gleeble-simulated ICCGHAZ specimens and specimens cut from the real weld specimens can be seen in Fig. 7. On average, impact toughness of the simulated ICCGHAZ improved by 8.4 J (25%). The difference was also statistically significant with 5% risk (*p* value of 0.024). The Charpy specimens with several different HAZ subzones below their notches saw an increase of 7.5 J (18%) on

Fig. 4 Cooling curves of the weld

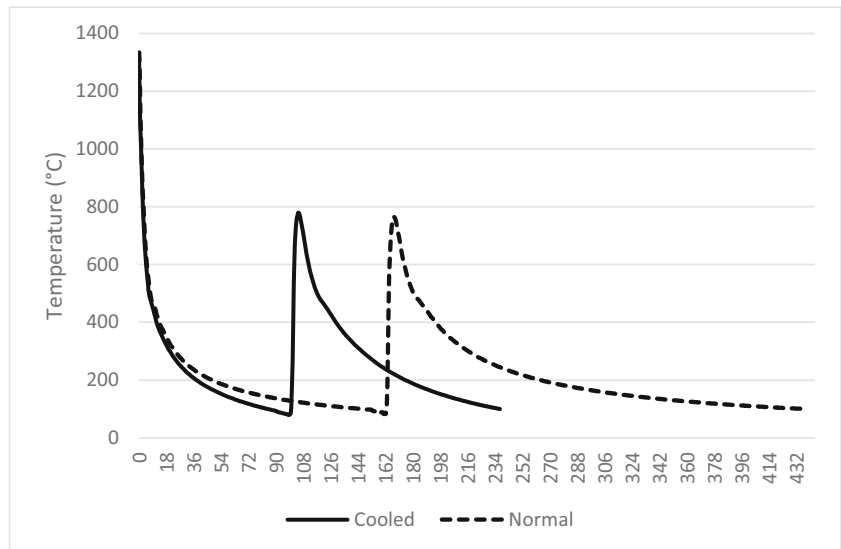


Fig. 5 Cooling times down to 500 °C

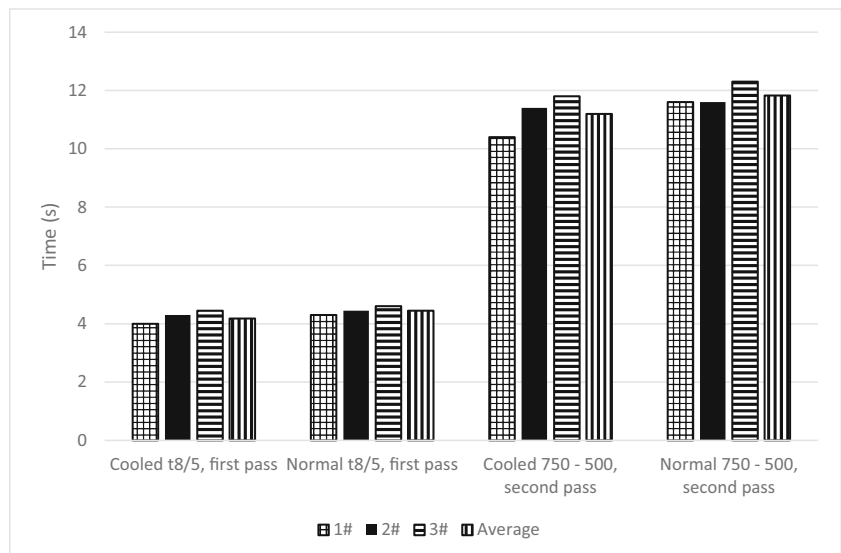


Fig. 6 Cooling times down to 100 °C

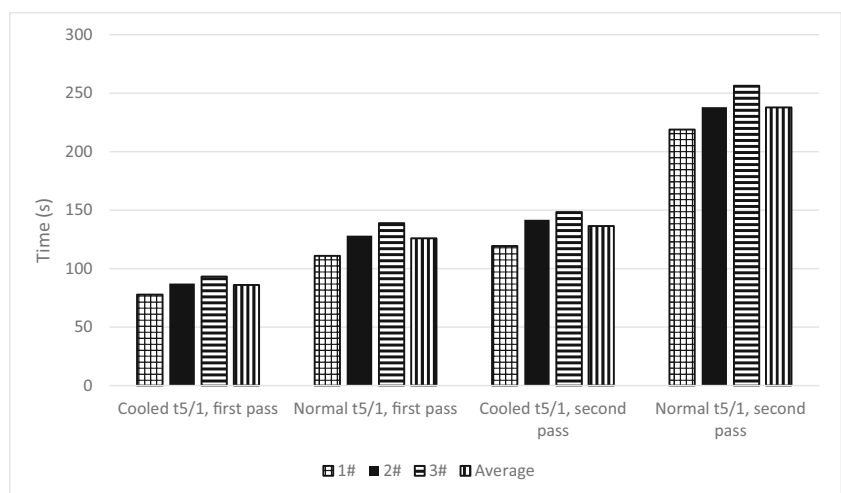


Table 6 Time saved by utilizing copper cooling blocks in the welding process

	Time saved on average
t8/5, first pass	0.27
t5/1, first pass	39.9
750–500, second pass	0.63
t5/1, second pass	101.3
Total	142.1

average with a p value of 0.027, indicating the result is significant as well.

The fracture surfaces of specimens from the cooled welds showed higher percentages of ductile fracture than the normal welds as can be seen in Fig. 8. The simulated ICCGHAZ specimens showed no scatter at all, and the fracture surface was 10% more ductile when the weld was cooled relative to the normal weld. The specimens from the real welds demonstrated some scat-

ter, but the difference between cooled and normal specimens was still significant with a p value of 0.005. The scatter found is likely to be caused by porosity or other defects that were caused by the welding process as the welded joint is not as homogeneous as a Gleeble-simulated microstructure. The mean percentage ductile fracture surface increased 27.5 percentage points from 35.0 to 62.5% as a result of the forced cooling.

3.3 Strength

A similar trend can be observed with the tensile tests as with the toughness tests, specimens from the cooled welds displayed superior properties compared to those from the normal welds. Both tensile and yield strength increased when the weld cooling was forced. On average, the tensile strength grew by 4.2% with a p value of 0.069, which means that the tensile strength might not actually be affected by the external cooling. However, it is more likely than not that it does since

Fig. 7 Mean impact toughness at -40 °C with error bars indicating one standard deviation. (Means of three specimens)

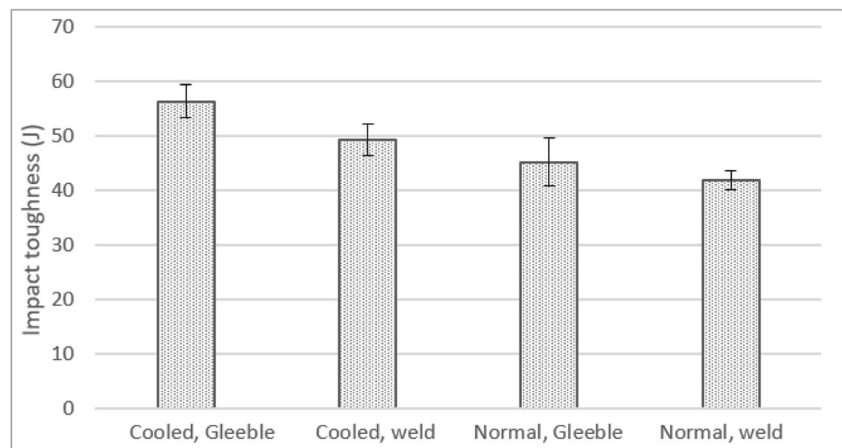
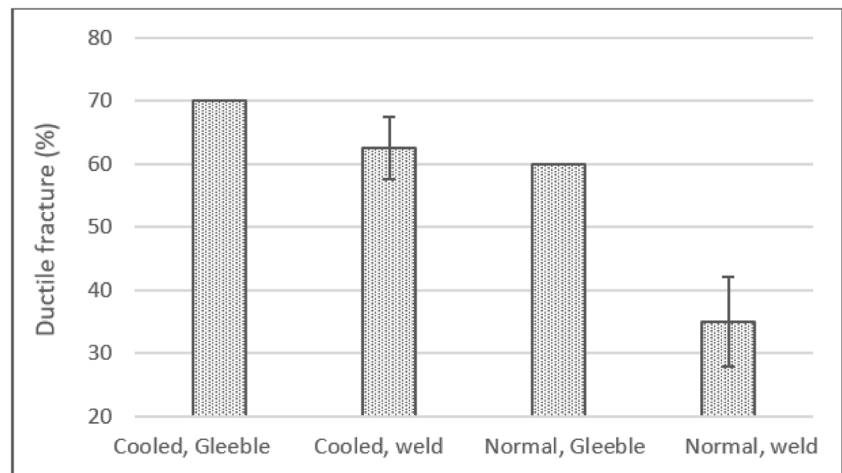


Fig. 8 Mean percentage ductile fracture with error bars indicating one standard deviation. (Means of three specimens. The Gleeble samples showed no scatter at all.)



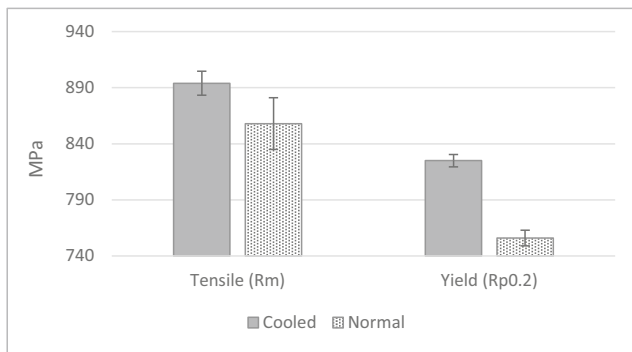


Fig. 9 Mean cross-weld tensile and yield strengths with error bars indicating one standard deviation. (Means of three specimens)

the p value is relatively small. Mean yield strength increased 9.1% with a p value of 0.00018 when external cooling was used. The increase in yield and tensile strength was in line with previous findings made by the authors on the CGHAZ of a 960-MPa steel in which the yield and tensile strength of the CGHAZ increased when the steel was cooled down to 100 °C with cooling rate of 15 °C/s [16] (Fig. 9).

Uniform elongation decreased slightly on average when external cooling was used, but as the magnitude of the elongation is only around 1%, the effect of the cooling on the elongation is not significant, since in both cases, elongation of this magnitude is poor. Furthermore, there was a lot of scatter in the results and the p value was 0.818, which means it cannot be claimed that the cooling has any kind of effect on the elongation (Fig. 10).

The cooling caused the yield strength to increase by a large margin without a matching increase in tensile strength, which led to the Y/T ratio suffering as a result of the forced cooling (Fig. 11). However, the difference is marginal since on average, the Y/T increased from 0.88 to 0.92.

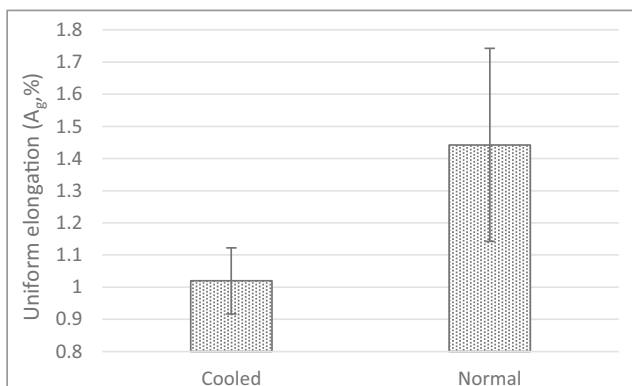


Fig. 10 Percent uniform elongation obtained on cross-weld tensile specimens with error bars indicating one standard deviation. (Means of three specimens)

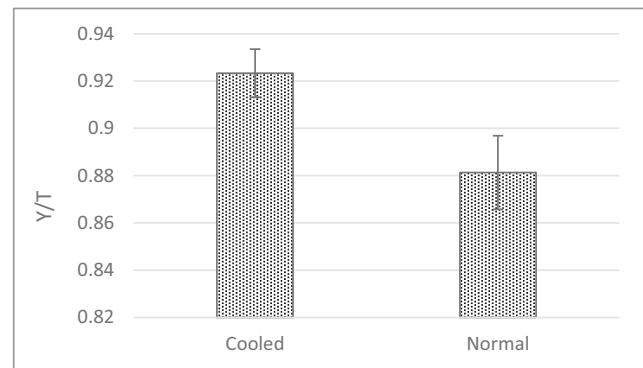


Fig. 11 Y/T-ratios of cross-weld tensile specimens with error bars indicating one standard deviation. (Means of three specimens)

3.4 Microstructure

The grain size of the specimens can be seen in Fig. 12. The grain size was calculated by using the mean linear intercept method, and it was confirmed that the cooling does not have a significant effect on the grain size of the ICCGAZ. Cooled specimens had a mean linear intercept grain size of about 46 μm while normal specimens had a mean linear intercept size of about 48 μm, but since there was lot of scatter in the grain sizes, the difference is not significant. The microstructure was mostly martensitic-bainitic in both cooled and normal specimens.

Figures 13 and 14 show the microstructures of the Gleeble-simulated ICCGAZ specimens more closely. Figure 13 displays the overall microstructure covering a few prior austenite grains while Fig. 14 shows a higher magnification image of the martensite-austenite (M-A) constituents seen around the prior austenite grain boundaries in Fig. 13. The main differences between the microstructures are that the ICCGAZ specimens that were rapidly cooled show a larger fraction of M-A constituents than the normally cooled specimens. This usually tends to make the steel more brittle, especially because the M-A constituents are necklaced, which can assist cleavage crack nucleation and propagation [11, 20], and therefore, this observation appears to be inconsistent with the better Charpy-V toughness of the simulated rapidly cooled ICCGAZ. On the other hand, the normally cooled specimens show a significantly larger fraction of carbides, and the carbides are larger than those in the rapidly cooled specimen. Carbides are known to be detrimental to the mechanical properties of the steel [21, 22]. Furthermore, the larger the carbides are, the more detrimental they are to the mechanical properties. It therefore appears that in the present case, the larger carbides are more detrimental to the Charpy-V toughness of the ICCGAZ than the M-A constituents. The faster cooling reduced the fraction of carbides and refined their size leading to superior Charpy-V toughness of the cooled specimens.

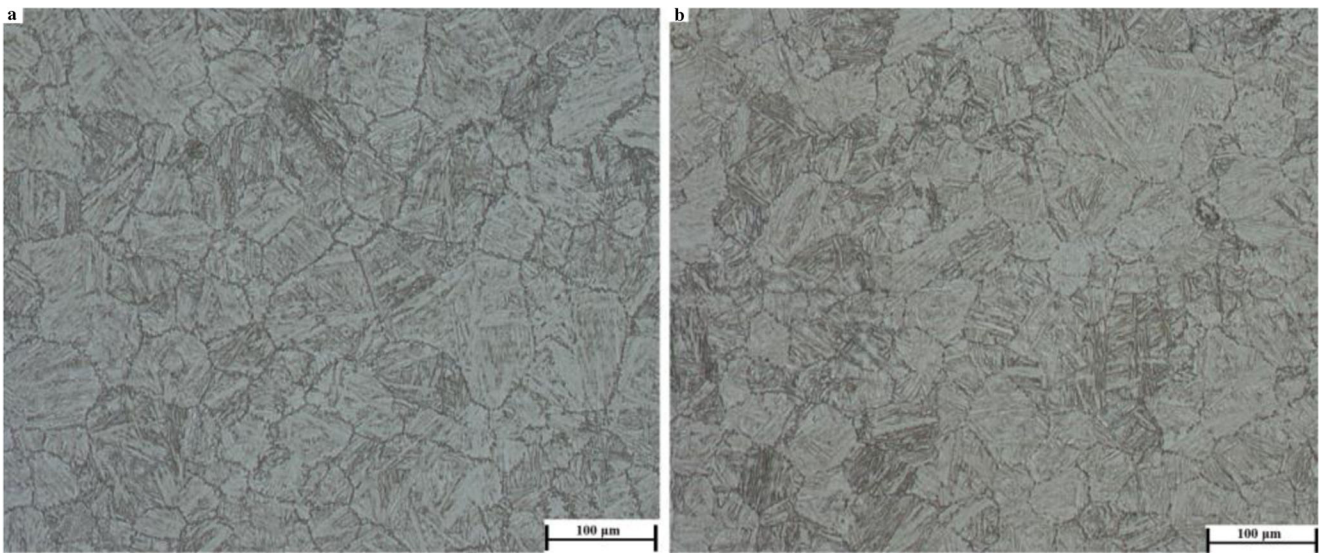


Fig. 12 Microstructural image of **a** cooled and **b** normal simulated ICCGHAZ specimen taken with optical microscope

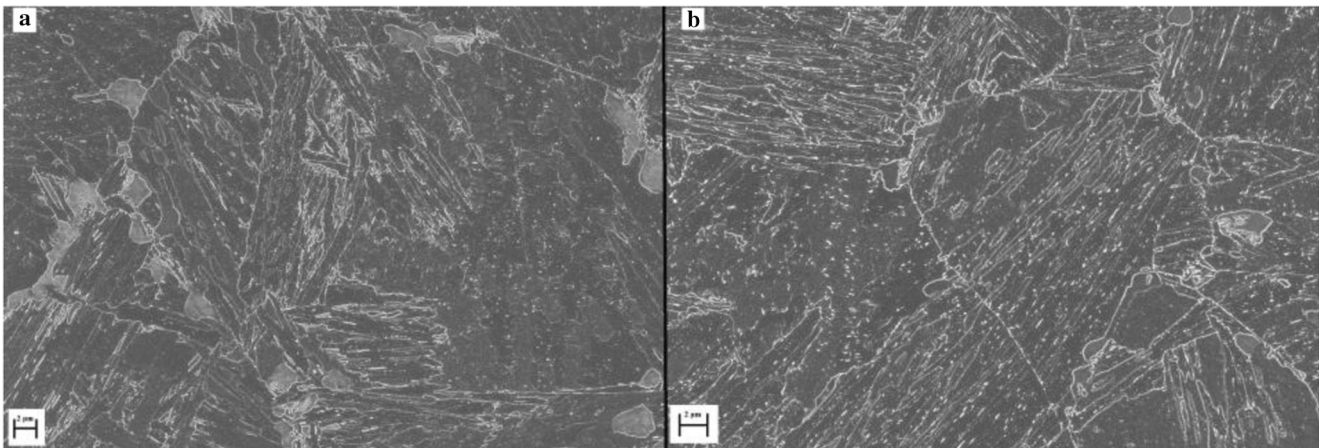


Fig. 13 Microstructural image of **a** cooled and **b** normal simulated ICCGHAZ specimens. FESEM SEI

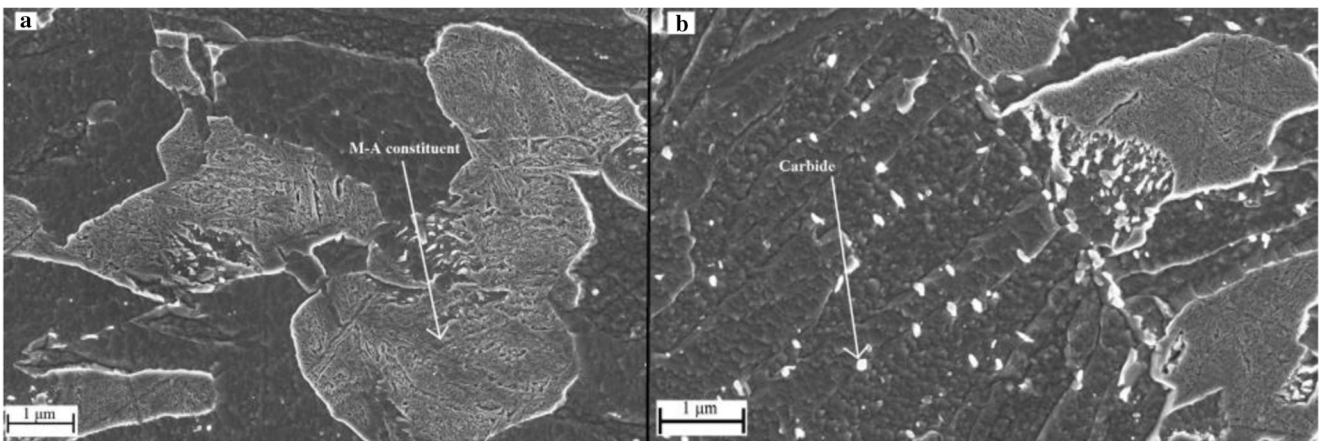


Fig. 14 Microstructural image of **a** cooled and **b** normal samples

4 Conclusion

From mechanical property point of view, it could be beneficial to introduce external cooling to the welding process when multipass welding is used, especially from the ICCGHAZ toughness point of view, as it improved significantly when the cooling of the weld was accelerated down to 100 °C. The increased impact toughness of the ICCGHAZ was caused by reducing the time carbides have to form and to grow, as the normal specimens had significantly more carbides in them and they were coarser than in the cooled specimens. In addition to the benefits to ICCGHAZ, previous research by authors has found that cooling to low temperatures has a similar effect on the CGHAZ of some ultrahigh- and high-strength steels, but in the CGHAZ, the differences were mostly caused by achieving smaller grain size [14, 15]. Furthermore, in this study, over 140 s was shaved off from two pass welding when the interpass temperature was 100 °C. This means that depending on heat input, material thickness, and number of weld passes, the waiting time could be reduced by tens of percent.

Acknowledgements Open access funding provided by University of Oulu including Oulu University Hospital. The authors are grateful for the financial support of the Business Finland and to Juha Uusitalo for conducting the Gleeble simulations used in this study.

OpenAccess This article is distributed under the terms of the Creative Commons Attribution 4.0 International License (<http://creativecommons.org/licenses/by/4.0/>), which permits unrestricted use, distribution, and reproduction in any medium, provided you give appropriate credit to the original author(s) and the source, provide a link to the Creative Commons license, and indicate if changes were made.

References

1. ArcelorMittal, Amstrong Ultra – Ultra high strength steels, <http://industry.arcelormittal.com/catalogue/A22/EN>, Accessed 22-01-2018
2. Javidan F, Heidarpour A, Zhao X-L, Hutchinson CR, Minkkinen J (2016) Effect of weld on the mechanical properties of high strength and ultra-high strength steel tubes in fabricated hybrid sections. *Eng Struct* 118:16–27. <https://doi.org/10.1016/j.engstruct.2016.03.046>
3. Qiang X, Jiang X, Bijlaard FS, Kolstein H (2016) Mechanical properties and design recommendations of very high strength steel s960 in fire. *Eng Struct* 112:60–70. <https://doi.org/10.1016/j.engstruct.2016.01.008>
4. SSAB, Welding of strenx, www.ssab.com/Products/Brands/Strenx/Products/Strenx-700-MC?tab=workshop, accessed: 2016-02-03
5. Chang L, Bhadeshia H (1996) Microstructure of lower bainite formed at large undercoolings below bainite start temperature. *Mater Sci Technol* 12:233–236. <https://doi.org/10.1179/02670839679016568>
6. Pirinen M (2013) The effects of welding heat input on the usability of high strength steels in welded structures. Dissertation, Lappeenranta University of Technology
7. Kim S, Kang D, Kim T-W, Lee J, Lee C (2011) Fatigue crack growth behavior of the simulated HAZ of 800 MPa grade high-performance steel. *Mater Sci Eng A* 528:2331–2338. <https://doi.org/10.1016/j.msea.2010.11.089>
8. Chen X-W, Liao B, Qiao G-Y et al (2013) Effect of Nb on mechanical properties of HAZ for high-Nb X80 pipeline steels. *J Iron Steel Res Int* 20:53–60. [https://doi.org/10.1016/S1006-706X\(13\)60216-2](https://doi.org/10.1016/S1006-706X(13)60216-2)
9. Jang J-I, Lee B-W, Ju J-B, Kwon D, Kim WS (2003) Experimental analysis of the practical LBZ effects on the brittle fracture performance of cryogenic steel HAZs with respect to crack arrest toughness near fusion line. *Eng Fract Mech* 70:1245–1257. [https://doi.org/10.1016/S0013-7944\(02\)00111-X](https://doi.org/10.1016/S0013-7944(02)00111-X)
10. Lan L, Kong X, Qiu C, Zhao D (2016) Influence of microstructural aspects on impact toughness of multi-pass submerged arc welded HSLA steel joints. *Materials Design* 90:488–498. <https://doi.org/10.1016/j.matdes.2015.10.158>
11. Wang X, Wang X, Shang C, Misra R (2016) Characterization of the multi-pass weld metal and the impact of retained austenite obtained through intercritical heat treatment on low temperature toughness. *Mater Sci Eng A* 649:282–292. <https://doi.org/10.1016/j.msea.2015.09.030>
12. Kim J, Yoon E (1998) Notch position in the HAZ specimen of reactor pressure vessel steel. *J Nucl Mater* 257:303–308. [https://doi.org/10.1016/S0022-3115\(98\)00451-6](https://doi.org/10.1016/S0022-3115(98)00451-6)
13. Wang XL, Tsai YT, Yang JR, Wang ZQ, Li XC, Shang CJ, Misra RDK (2017) Effect of interpass temperature on the microstructure and mechanical properties of multi-pass weld metal in a 550-MPa-grade offshore engineering steel. *Welding in the World* 61:1155–1168. <https://doi.org/10.1007/s40194-017-0498-x>
14. Peng Y, Wang AH, Xiao HJ, Tian ZL (2012) Effect of interpass temperature on microstructure and mechanical properties of weld metal of 690 MPa HSLA steel. *Mater Sci Forum* 706-709:2246–2252. <https://doi.org/10.4028/www.scientific.net/msf.706-709.2246>
15. Laitila J, Larkiola J, Porter D (2017) Effect of forced cooling on the tensile properties and impact toughness of the coarse-grained heat-affected zone of a high-strength structural steel. *Welding in the World* 62:79–85. <https://doi.org/10.1007/s40194-017-0532-z>
16. Laitila J, Larkiola J, Porter D (2018) Effect of forced cooling after welding on CGHAZ mechanical properties of a martensitic steel. *Welding in the World* 62:1247–1254. <https://doi.org/10.1007/s40194-018-0617-3>
17. Sung HK, Lee DH, Shin SY et al (2015) Effect of finish cooling temperature on microstructure and mechanical properties of high-strength bainitic steels containing Cr, Mo, and B. *Mater Sci Eng A* 624:14–22. <https://doi.org/10.1016/j.msea.2014.11.035>
18. Gavzdyl J. (2001) Cryogenic weld cooling. *Industrial Laser Solutions For Manufacturing*. <http://www.industrial-lasers.com/articles/print/volume-17/issue-5/features/cryogenic-weld-cooling.html>. Accessed 23.08.2018
19. Strenx 960 MC – high-strength structural steel at 960 MPa - SSAB, <http://www.ssab.com/products/brands/strenx/products/strenx-960-mc>. Accessed 23.08.2018
20. Wang X, Nan Y, Xie Z et al (2017) Influence of welding pass on microstructure and toughness in the reheated zone of multi-pass weld metal of 550 MPa offshore engineering steel. *Mater Sci Eng A* 702:196–205. <https://doi.org/10.1016/j.msea.2017.06.081>
21. Li J, Zhang C, Liu Y (2016) Influence of carbides on the high-temperature tempered martensite embrittlement of martensitic heat-resistant steels. *Mater Sci Eng A* 670:256–263. <https://doi.org/10.1016/j.msea.2016.06.025>
22. Sun G, Yao S, Wang Z et al (2018) Microstructure and mechanical properties of HSLA-100 steel repaired by laser metal deposition. *Surf Coat Technol* 351:198–211. <https://doi.org/10.1016/j.surfcoat.2018.07.048>